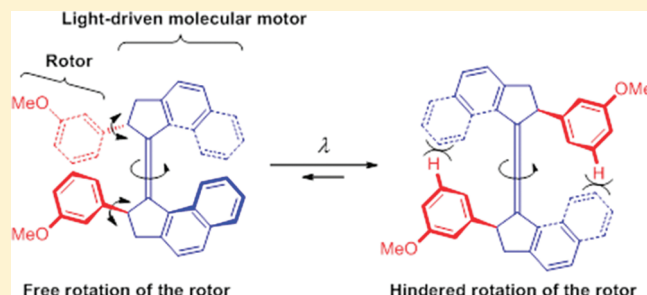# Control of Rotor Function in Light-Driven Molecular Motors

Anouk S. Lubbe, Nopporn Ruangsupapichat, Giuseppe Caroli, and Ben L. Feringa*

Centre for Systems Chemistry, Stratingh Institute for Chemistry and Zernike Institute for Advanced Materials, University of Groningen, Nijenborgh 4, Groningen 9747AG, The Netherlands

**S** *Supporting Information*

**ABSTRACT:** A study is presented on the control of rotary motion of an appending rotor unit in a light-driven molecular motor. Two new light driven molecular motors were synthesized that contain aryl groups connected to the stereogenic centers. The aryl groups behave as bidirectional free rotors in three of the four isomers of the 360° rotation cycle, but rotation of the rotors is hindered in the fourth isomer. Kinetic studies of both motor and rotor functions of the two new compounds are given, using $^1$H NMR, 2D-EXSY NMR, and UV—vis spectroscopy. In addition, we present the development of a new method for introducing a range of aryl substituents at the $\alpha$-carbon of precursors for molecular motors. The present study shows how the molecular system can be photochemically switched between a state of free rotor rotation and a state of hindered rotation and reveals the dynamics of coupled rotary systems.

## ■ INTRODUCTION

Molecular motors are ubiquitous throughout nature and perform essential tasks in biological systems.[1] Well-known examples are bacterial flagella,[2] kinesine and myosin,[3] and ATPase motors.[4] These intricate natural molecular motors have been a source of inspiration for the development of a variety of artificial molecular mechanical devices,[5] including switches,[16,7] shuttles, muscles, and rotary and translational motors.[5] Because potential applications are highly diverse, artificial molecular motors are considered extremely useful in powering future nanodevices.[8] Dynamic control of a myriad of functions, transmission of motion in multicomponent systems, and out-of-equilibrium assembly are important perspectives offered by rotary molecular motors. Various approaches toward synthetic rotary motors have been reported, especially systems powered by light[9] and chemical energy.[10] A particularly versatile design is based on chiral overcrowded alkenes. The "first-generation" light-driven molecular motor **1** (Figure 1) consists of two identical chromophores linked through a central alkene,[11] which serves as the axle of rotation. This motor contains two stereogenic centers with methyl substituents in pseudoaxial orientation and the directionality of the rotary motion of **1** is governed by the chirality at these stereogenic centers in the helical molecule.

With this system, the unidirectional 360° rotation of the upper half relative to the lower half in the molecular motor is performed through a four-step switching cycle. There are two irradiation steps (energetically uphill), during which photochemical *cis—trans* isomerization occurs, forcing the methyl substituents in an unfavorable pseudoequatorial position. Each photoisomerization step is followed by an irreversible thermal isomerization step (energetically downhill) that re-establishes the favorable pseudoaxial

orientation of the methyl substituents. The four-step cycle provides full 360° unidirectional rotation of one-half of the molecule with respect to the other. Since the introduction of motor **1**, several advanced light-driven molecular motors have been designed and their dynamic properties studied.[12] To investigate the unidirectional rotation of the overcrowded alkene in more detail, the size of the substituent next to the double bond was varied in "second-generation" molecular motors.[13] Exchanging the methyl group in the second-generation motor for a more sterically demanding phenyl group at the stereogenic center in motor **2** (Figure 1) only slightly increased the barrier for the thermal helix inversion step ($t_{1/2}$ = 9.8 min at rt) compared to that in the corresponding methyl substituted analogue ($t_{1/2}$ = 3.2 min at rt). Light-driven molecular motor **2** was found particularly suitable to demonstrate transmission of motion to control the organization of a supramolecular system and to perform work. Specifically, the photochemical and thermal isomerizations involved with motor **2**, embedded as chiral dopant in a liquid crystal (LC) film, were used to induce the rotational reorganization of LC surface textures and rotate a microscale object on top of the LC film.[14] Moreover, it was found that motor **2** with a phenyl substituent has a higher helical twisting power and enhanced ability to control the direction of rotational reorganization of the LC's surface texture compared to the corresponding motor with a methyl substituent.[14b]

Another notable example of a functional molecular motor is the so-called "molecular gearbox" motor **3** (Figure 1).[15] In this system, two rotary units are present, representing two coupled dynamic functions. Molecule **3** contains a freely rotating
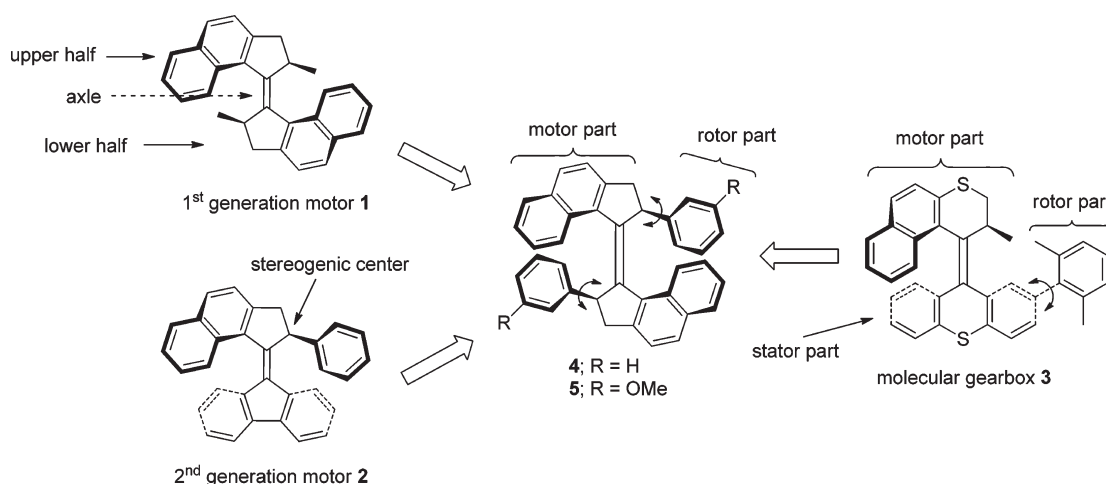
**Figure 1.** Design features of first- and second-generation rotary motors and coupled rotary systems: first-generation molecular motor **1**, second-generation motor **2** with phenyl substituent at the stereogenic center, "molecular gearbox" **3**, and molecular motors **4** and **5** with phenyl and *m*-methoxyphenyl groups at the stereogenic centers, respectively.

**Scheme 1. New Synthetic Pathway for the α-Aryl Ketone Upper-Half**
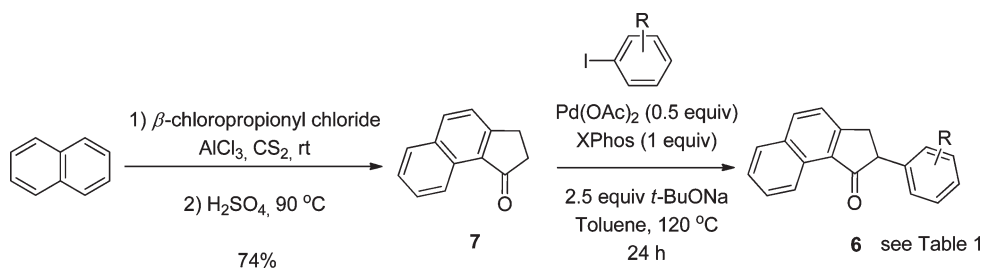


1,5-dimethylphenyl group attached to the stator unit, which behaves as a bidirectional rotor unit.[5] It was found that the rate of rotation of the rotor moiety (1,5-dimethylphenyl) in this molecular system was different for each of the four isomers formed during a full 360° rotary cycle of the motor. This rotor control is considered an important step in the development of future coupled rotary systems.[6] In these two examples, the aromatic group in the motor structure has played an important role to perform distinct functions. A major question arises regarding the first-generation motors: if the methyl groups in **1** are replaced by aromatic groups (as in **4** and **5**) at the stereogenic centers of a first-generation molecular motor (Figure 1), will it still be possible to control coupled dynamic functions as described above?
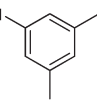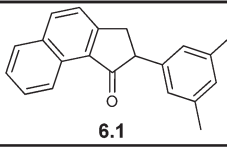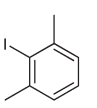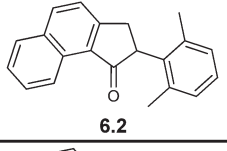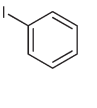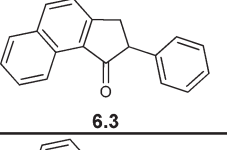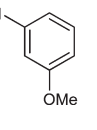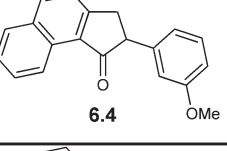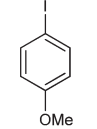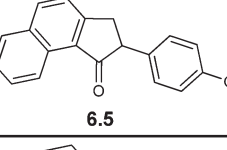
We present here new molecular motors **4** and **5** to address this pertinent question and to further study the dynamic properties of coupled rotary systems. Both of these molecules were designed based on the structures **1**−**3**, but for motor **4** the methyl groups are exchanged for phenyl groups, and for **5** *m*-methoxyphenyl groups are present at the stereogenic centers (structures **4** and **5** illustrate the modifications introduced to first-generation motor **1**, Figure 1). These aryl substituents are expected to behave as bidirectional rotors, as observed for motor **3**. Using UV−vis and temperature-dependent NMR spectroscopy, we are able to show that **4** and **5** function as first-generation motors and that in these molecules the rotation of the rotor part is coupled to the unidirectional rotation of the motor part. The design of motors

**4** and **5** is anticipated to provide a convenient handle for analyzing the rotation of the rotor moiety (at the stereogenic center) using dynamic (EXSY) NMR experiments. In this paper, we focus on studies toward the rate of rotation ($k$) of the rotor moiety including the behavior of light-driven rotary molecular motors. Likewise, we present a study toward the development of a new method for introducing a range of new substituents at the α-carbon of ketones (precursors for molecular 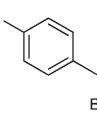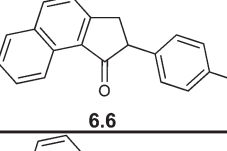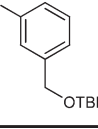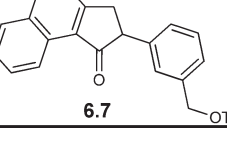motors). This new design is the key to achieving conclusive evidence of the coupled rotation while still preserving the proper light-driven motor function.

## ■ RESULTS AND DISCUSSION

In our synthetic approach toward target molecules **4** and **5**, we anticipated developing a short procedure to prepare a number of different α-aryl substituted ketones **6** as precursors being part of a more general route to "first-generation" aryl-substituted molecular motors. As we reported previously, the upper-half α-phenyl ketone **6.3** (Scheme 1) can be synthesized in six steps (in an overall yield of 30%) from methyl 2-bromo-2-phenylacetate.[13] This procedure does not allow for facile synthesis of motors with different aryl substituents introduced at the α-position. Here, we present a new synthetic route toward various α-aryl substituted ketones **6**. This new route consists of two steps and therefore allows us to easily vary the aryl substituents at the α-position. Consequently, several α-aryl-substituted ketones **6** have been synthesized and the reaction conditions have been optimized.

**Table 1. $\alpha$-Arylation Reaction Using Pd(OAc)$_2$ and XPhos with Different Aryl Halides**

| Entry | Aryl Halide | Product | %Yield |
|---|---|---|---|
| 1[a] | | 6.1 | 62 |
| 2 | | 6.2 | 67 |
| 3 | | 6.3 | 70 |
| 4[a] | | 6.4 | 42 |
| 5 | | 6.5 | 13 |
| 6 | | 6.6 | - |
| 7[b] | | 6.7 | 64 |

[a] Smaller amounts of Pd(OAc)$_2$/XPhos (1/2 mol %, 5/10 mol % and 20/40 mol %) did not result in product formation or produced poor yields. [b] The aryl halide was prepared in one step from iodobenzyl alcohol with *tert*-butyldiphenylsilyl chloride (*t*-BDPSCl).

Although the development of an efficient method for the formation of a bond between an aryl moiety and the $\alpha$-carbon of a carbonyl compound has long been a challenging problem in organic synthesis, Buchwald[16] and co-workers have reported the $\alpha$-arylation of ketones via palladium catalyzed reaction. This methodology forms the basis for the shorter synthetic route toward $\alpha$-aryl substituted ketones **6** described here.

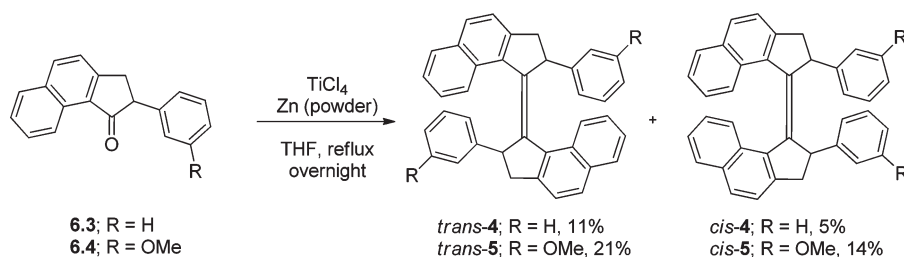The two-step synthetic approach toward the desired $\alpha$-aryl-substituted ketones is shown in Scheme 1. The first step involves a Friedel–Crafts acylation of the naphthalene with $\beta$-chloropropionyl chloride, leading to ketone **7**. The results of the subsequent Pd-catalyzed $\alpha$-arylation reaction using XPhos[17] as ligand for a variety of conditions and aryl compounds are shown in Table 1.

In order to establish the optimal arylation conditions (Table 1), the amount of Pd/XPhos was varied (Table S1, Supporting Information). The use of 50/100 mol % of Pd/XPhos resulted in arylation of 1-iodo-3,5-dimethylbenzene,

1-iodo-2,6-dimethylbenzene, and iodobenzene to provide $\alpha$-aryl ketones **6.1**–**6.3** in yields up to 70% (entries 1–3). We have also observed the arylation reaction with an electron donating group (EDG) present at the phenyl moiety, as shown for *m*- and *p*-iodoanisole (entries 4 and 5). It is evident that the arylation reaction is dependent on the position of the methoxy group on the aryl halide reagent. The use of *p*-iodobenzyl bromide, which has acidic benzylic protons, resulted in side products (possibly from the S$_N$2 reaction) rather than the desired product (entry 6). In order to further functionalize the aryl moiety, we have also performed the arylation reaction with *tert*-butyl(3-iodobenzyloxy) diphenylsilane, providing aryl ketone **6.7** in 64% (entry 7).

These results illustrate that it is possible to synthesize the $\alpha$-arylated ketone upper-half in two steps from naphthalene. Future optimization of this new procedure, especially for large-scale synthesis, is required in view of the rather large amount of palladium catalyst and ligand that is used in the $\alpha$-arylation reaction. Although these arylation reactions so far need a higher

**Scheme 2. Synthesis of "First-Generation" Light-Driven Molecular Motors 4 and 5**



**6.3**; R = H
**6.4**; R = OMe

TiCl$_4$
Zn (powder)

THF, reflux
overnight

*trans*-**4**; R = H, 11%
*trans*-**5**; R = OMe, 21%

*cis*-**4**; R = H, 5%
*cis*-**5**; R = OMe, 14%

**Scheme 3. Rotary Cycle of "First-Generation" Molecular Motor 4**



step 1
$\lambda \geq 365$ nm
at -50 °C

stable *cis*-**4**

unstable *trans*-**4**

step 4
at 30 °C

step 2
at 0 °C

step 3
$\lambda \geq 365$ nm
at rt

unstable *cis*-**4**

stable *trans*-**4**
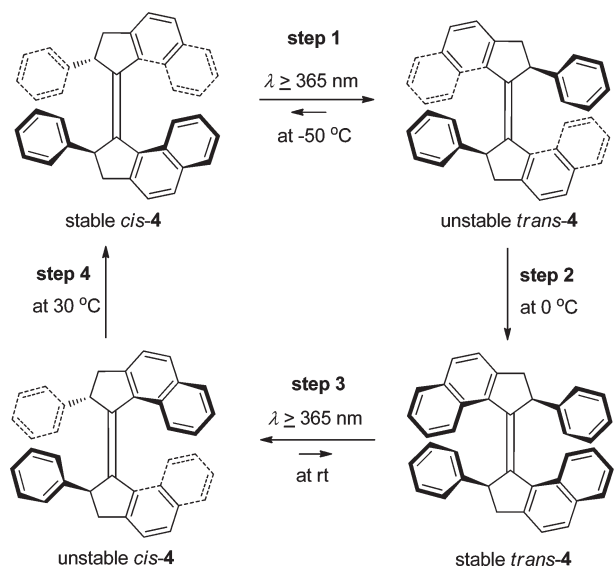
loading of palladium catalyst and ligand than anticipated,[16] it is a significantly more efficient route than the original six-step procedure in terms of yield and time.[13] Moreover, we found it to be a valuable alternative for small scale synthesis to access a range of different $\alpha$-aryl substituted ketones suitable as molecular motor precursors to be tested in several applications.

**Synthesis of the Molecular Motors.** Because of severe steric hindrance in the structures of **4** and **5**, most olefination reactions are not suitable for the formation of the central olefinic bond in these molecules. We were pleased to find that sterically overcrowded alkenes **4** and **5** were prepared in one step by a McMurry coupling reaction of the corresponding ketone as shown in Scheme 2. Ketones **6.3** and **6.4** were coupled in the presence of TiCl$_4$ and zinc powder by refluxing in THF overnight, providing alkene **4** in 16% yield and alkene **5** in 35% yield, both as a mixture of *cis* and *trans* isomers.

Separation of the isomers of motors **4** and **5** was achieved with flash column chromatography and provided pure stable *cis*-**4** (5%) and stable *trans*-**4** (11%) and pure stable *cis*-**5** (14%) and stable *trans*-**5** (21%), respectively. The assignment of the structures of *cis* and *trans* **4** and **5** is based on related "first-generation" motors and is supported by calculations (Figures S1 and S2, Supporting Information). To analyze the light-driven motor function, the photochemical and thermal behavior of compounds **4** and **5** as determined by UV–vis spectroscopy, kinetic analysis

and $^1$H NMR spectroscopy is first described. This is followed by a study of the rotation of the aryl moieties (the rotor function) of these compounds by 2D-EXSY NMR spectroscopy.

**Photochemical and Thermal Behavior of Molecular Motor 4.** The overcrowded alkene **4** can undergo a full 360° unidirectional rotation of one-half of the molecule relative to another half upon irradiation followed by a thermal helix inversion process (Scheme 3).

The thermal and photochemical steps in the rotation process of **4** were studied by $^1$H NMR spectroscopy. Figure 2a shows the spectrum of a solution of stable *cis*-**4** in dichloromethane-$d_2$ at −50 °C. Distinctive features are absorptions of the aliphatic protons H$_a$, H$_b$, and H$_c$. Only negligible coupling is expected between H$_a$ and H$_b$. Therefore, the absorption at 3.9 ppm is assigned to H$_c$. As the coupling constant is expected to be larger for geminal protons than for vicinal protons, the absorption at 2.9 ppm ($J = 15.4$ Hz) is assigned to H$_b$, and the absorption at 4.5 ppm ($J = 6.9$ Hz) is assigned to H$_a$.

Irradiation at $\lambda \geq 365$ nm of the solution of stable *cis*-**4** (at −75 °C) resulted in the formation of a new isomer, assigned unstable *trans*. All absorptions shifted, most notably the doublet absorptions at 2.9 ppm (H$_b$) and 3.9 ppm (H$_c$). These absorptions are shifted downfield and upfield, respectively, and appear together as two multiplets at 3.3 and 3.5 ppm. Extended irradiation results in a photoequilibrium which strongly favors the formation of unstable *trans*-**4** (92:8, unstable *trans*/stable *cis*) as is evident from the $^1$H NMR spectra shown in Figure 2a,b. An interesting observation is that in Figure 2b all five protons of the phenyl moiety absorb at a different chemical shift (four in the region 6.4–6.7, one at 7.25 ppm). This indicates that the phenyl group is not rotating freely.

Subsequently, the sample was heated to 0 °C for 15 min to induce thermal helix inversion, whereby the conformational strain due to the pseudoequatorial orientation of the phenyl moiety in unstable *trans*-**4** is released. A $^1$H NMR spectrum was recorded at −50 °C (Figure 2c). Again, all absorptions shifted and the absorptions of H$_b$ and H$_c$ can be found at 2.7 ppm (d, H$_b$) and 3.5 ppm (m, H$_c$), and the new isomer is assigned stable *trans*-**4**. In this isomer, the phenyl groups at the stereogenic center adopt a favored pseudoaxial orientation.

The sample was irradiated for a second time ($\lambda \geq 365$ nm, 4 h, −75 °C), and a $^1$H NMR spectrum was recorded at −50 °C (Figure 2d). All absorptions shifted again, and no residual stable *trans*-**4** was visible, implying full conversion. The absorptions of H$_b$ and H$_c$ can be found as two multiplets at 3.3 and 3.5 ppm, and the new isomer is assigned unstable *cis*-**4** (unstable *cis* > 95/stable *trans* < 5). It is noted that for this isomer, as well as in stable *cis*-**4** and stable *trans*-**4**, the absorptions of the phenyl moiety appear as a single peak at ∼7.2 ppm, implying free rotation around the
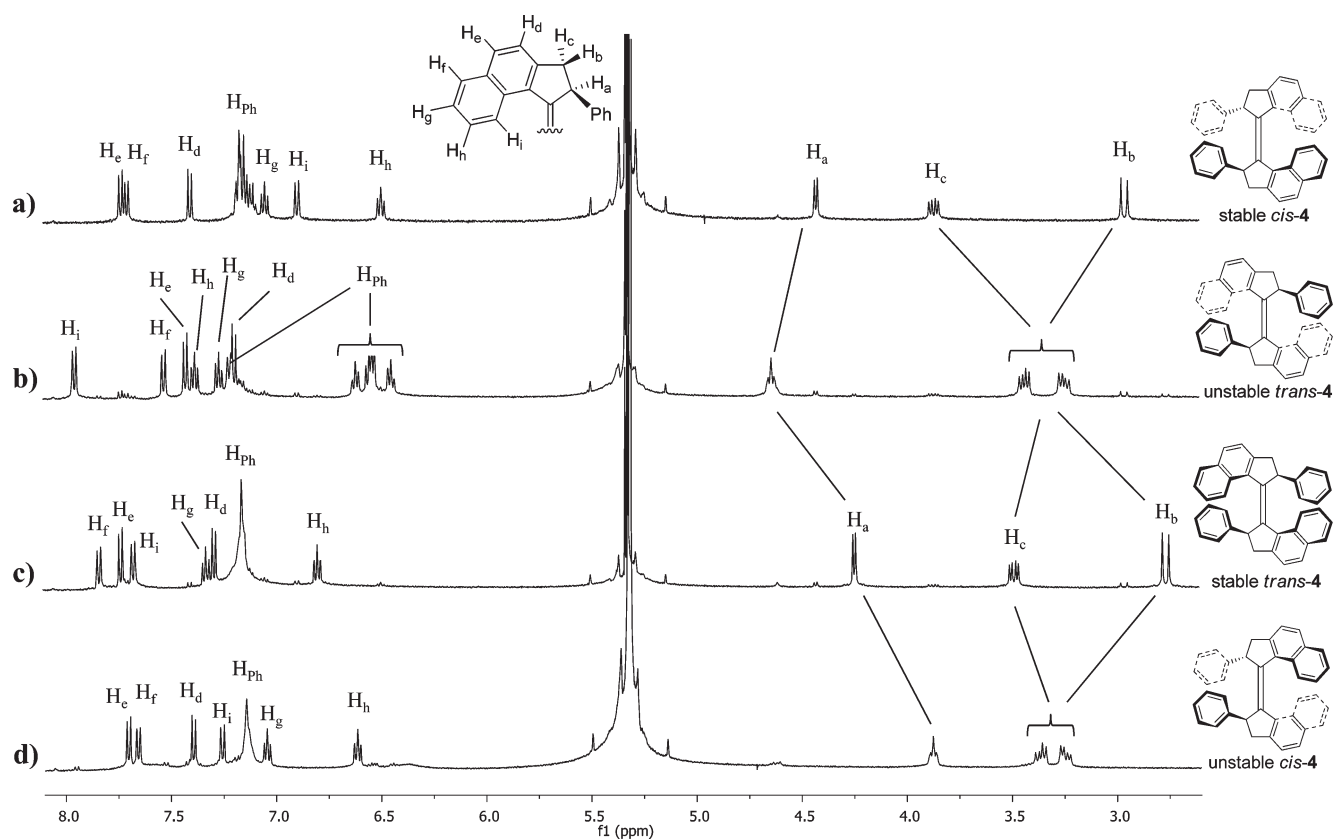
**Figure 2.** $^1$H NMR spectra (500 MHz) of **4** in CD$_2$Cl$_2$: (a) stable *cis*-**4**; (b) unstable *trans*-**4** formed upon photochemical isomerization ($\lambda \geq 365$ nm); (c) stable *trans*-**4** obtained after thermal helix inversion of unstable *trans*-**4** at rt; (d) unstable *cis*-**4** formed upon irradiation ($\lambda \geq 365$ nm) (all spectra were recorded at −50 °C).

single bond connecting the phenyl group to the stereogenic center of **4**. A second thermal helix inversion (30 °C, 30 min) ultimately regenerated stable *cis*-**4** (spectrum Figure 2a), thereby completing the 360° rotation around the central double bond.

Kinetic analysis was performed on both thermal helix inversions. For unstable *trans*-**4** → stable *trans*-**4**, $\Delta^{\ddagger}G°$ was calculated to be 78 kJ·mol$^{-1}$ ($t_{1/2}$ = 9.4 s at rt), and for unstable *cis*-**4** → stable *cis*-**4**, $\Delta^{\ddagger}G°$ = 98 kJ·mol$^{-1}$ ($t_{1/2}$ = 8.2 h at rt) was obtained. These data reveal that the half-life ($t_{1/2}$ = 9.4 s) of unstable to stable *trans*-**4** is not very different compared to the analogue with the methyl substituent (unstable *trans*-**1** → stable *trans*-**1**) at the stereogenic center ($t_{1/2}$ = 18 s at rt).[11] In contrast, the thermal isomerization step of unstable *cis*-**4** to stable *cis*-**4** ($t_{1/2}$ = 8.2 h at rt) is much slower than the corresponding isomerization of the analogous unstable *cis*-**1** → stable *cis*-**1** ($t_{1/2}$ = 74 min at rt).

An interesting feature of this motor **4** is that free rotation of the phenyl "rotor" moiety (at the stereogenic center) is observed in three of the four isomers (stable *cis*-, stable *trans*-, and unstable *cis*-) during a 360° cycle, but the rotation is hindered in the fourth isomer (unstable *trans*-**4**). $^1$H NMR data of motor **4** show that the free rotation of the phenyl group is hindered in the unstable *trans* isomer because of the significant steric hindrance of the naphthalene moiety in the opposite half of the motor. This is the reason why five protons of the phenyl rotor moiety in unstable *trans*-**4** show five distinct absorptions as shown in Figure 2b; the rotation is slow at the NMR time scale as compared with the other isomers. In stable *cis*-, stable *trans*- and unstable *cis*-**4** all the five protons of the phenyl "rotor" moiety are observed as a single

absorption (Figure 2a,c,d). Consequently, the phenyl substituent of motor **4** might be used as a switching system (between free and slow rotation) accompanying the motor switching between the stable *cis* and unstable *trans* isomers.

Unfortunately, because of overlap in the aromatic region of the $^1$H NMR spectrum between the absorptions of the rotor (phenyl) and the absorptions of the naphthalene moieties, the rotor properties could not be studied in more detail. Further research into the rotation of the bidirectional rotor was therefore conducted on molecular motor **5**, which has a methoxy-substituted rotor unit.

**Photochemical and Thermal Behavior of Molecular Motor 5.** Before studying the dynamic properties of the rotor part (*m*-methoxyphenyl) of motor **5**, the motor function itself was examined. Initial studies on the behavior of the motor unit were performed with the stable isomers[18] of *cis*-**5** and *trans*-**5** and the photochemical isomerization and thermal helix inversion processes were analyzed by UV−vis and $^1$H NMR spectroscopy. Likewise, it was anticipated that motor **5** should function as a light-driven molecular rotary motor which proceeds through a four-step switching cycle, similar to the cycle of motor **4** (Scheme 3).

A solution of stable *cis*-**5** (3.7 × 10$^{-5}$ M) in dichloromethane and a solution of stable *trans*-**5** (3.0 × 10$^{-5}$ M) in 1,2-dichloroethane[19] were used for the UV−vis spectroscopic studies. Starting with stable *cis*-**5** at −20 °C, a photochemical isomerization (with UV light ≥ 365 nm) generates unstable *trans*-**5** and the UV−vis absorption spectrum was measured at regular intervals until the photostationary state (PSS) was reached. An
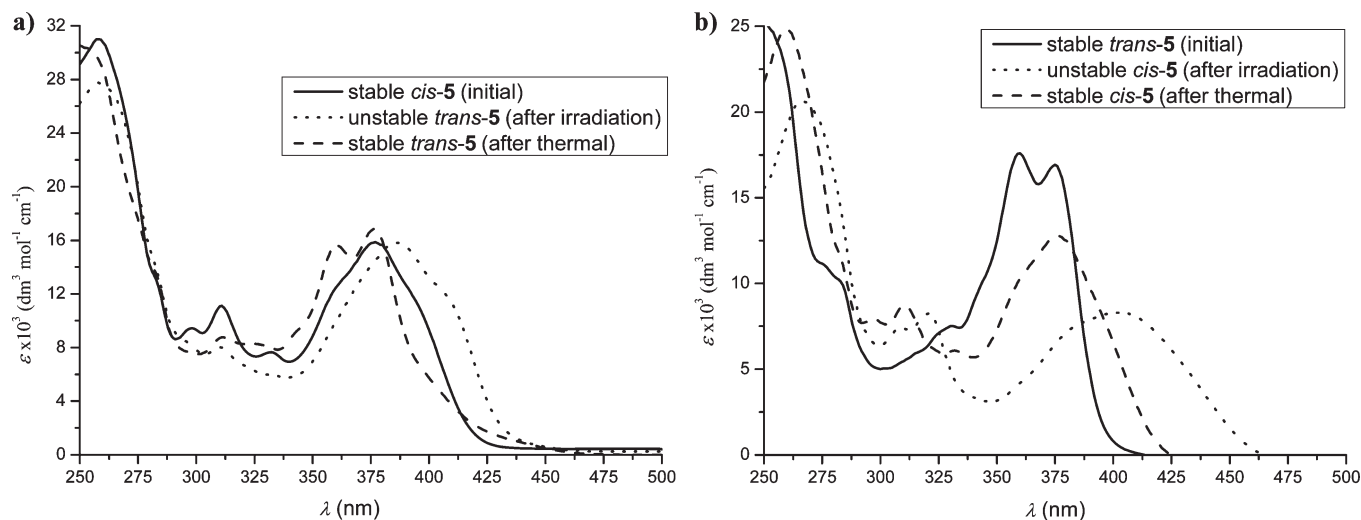
**Figure 3.** UV—vis spectra of molecular motor **5**: (a) photoisomerization and thermal helix inversion steps from stable *cis*- to stable *trans*-**5**; (b) photoisomerization and thermal helix inversion steps from stable *trans*- to stable *cis*-**5**.

isosbestic point was formed at 380 nm and a red-shift of the maximum at 375 nm ($\varepsilon = 15.8 \times 10^3$ dm$^3\cdot$mol$^{-1}\cdot$cm$^{-1}$) (to 387 nm ($\varepsilon = 15.8 \times 10^3$ dm$^3\cdot$mol$^{-1}\cdot$cm$^{-1}$)) was observed. The bathochromic shift can be attributed to the generation of an unstable *trans* isomer, where the ground state is destabilized compared to the stable *trans* isomer due to increased strain.[11] This decreases the energy gap, as seen with other first-generation molecular motors (dotted line, Figure 3a). The sample was then left for 100 min at −20 °C to allow the thermal helix inversion process to occur. The UV—vis spectrum indicates that the unstable *trans*-**5** has converted to stable *trans*-**5** ($\lambda_{max} = 375$ nm, $\varepsilon = 16.8 \times 10^3$ dm$^3\cdot$mol$^{-1}\cdot$cm$^{-1}$, dashed line, Figure 3a). On the basis of these data it can be concluded that one-half of the rotary cycle (180°) has been completed (stable *cis* → stable *trans*). Figure 3b shows the UV—vis spectra of the isomers observed during the other half of the 360° rotary cycle from stable *trans*-**5** via unstable *cis*-**5** to stable *cis*-**5**. A UV—vis spectrum of stable *trans*-**5** was acquired at rt. As expected, this spectrum (Figure 3b, solid line) is similar to the spectrum obtained after the thermal isomerization step as shown in Figure 3a (dashed line).

The solution of stable *trans*-**5** ($\lambda_{max} = 360$ nm, $\varepsilon = 17.6 \times 10^3$ dm$^3\cdot$mol$^{-1}\cdot$cm$^{-1}$) was then irradiated with UV light ($\geq 365$ nm) at 40 °C until the PSS was reached. In the UV—vis spectrum of unstable *cis*-**5** ($\lambda_{max} = 401$ nm, $\varepsilon = 8.3 \times 10^3$ dm$^3\cdot$mol$^{-1}\cdot$cm$^{-1}$, dotted line, Figure 3b), the expected red-shift was observed once again and a clear isosbestic point was displayed at 385 nm. Subsequently, the sample was left at 40 °C for 5 h. The final spectrum ($\lambda_{max} = 377$ nm, $\varepsilon = 12.8 \times 10^3$ dm$^3\cdot$mol$^{-1}\cdot$cm$^{-1}$, dashed line, Figure 3b) is similar to the spectrum of stable *cis*-**5** in Figure 3a (solid line) and it can be concluded that the other half of the 180° rotary cycle has been completed. However, the spectra of stable *cis* shown in Figure 3b (dashed line) and Figure 3a (solid line) are not completely identical, as was also observed for stable *trans* (Figure 3a, dashed line and Figure 3b, solid line). This indicates that, although the isomerization step proceeds as expected, the conversion in both halves of the cycle is less than 100%. Further ^{1}H NMR studies will provide more information about the actual conversion during the photochemical and thermal isomerization processes (vide infra).

In addition, UV—vis spectroscopy was used to study the kinetics of the two thermal isomerization steps. The changes in UV—vis absorption at 410 nm were monitored as a function of time at different temperatures (−5, −10, −12, −15, and −20 °C for unstable *trans*-**5** → stable *trans*-**5**; 30, 40, 50, and 60 °C for unstable *cis*-**5** → stable *cis*-**5**). Using these data, an Eyring plot was made for both thermal steps, from which the half-life and Gibbs free energy of activation were calculated. It was found that $t_{1/2} = 9.45$ s at rt ($\Delta^{\ddagger}G^{\circ} = 78.14$ kJ$\cdot$mol$^{-1}$; see Figure S3a, Supporting Information) for the isomerization of unstable *trans*-**5** to stable *trans*-**5**, a value similar to that of the analogous helix inversion of the related motor **4** which was determined to be 9.4 s at rt. The $t_{1/2}$ of unstable *cis*-**5** to stable *cis*-**5** is 6.2 h ($\Delta^{\ddagger}G^{\circ} = 97$ kJ$\cdot$mol$^{-1}$, at rt) (see Figure S3b, Supporting Information). This thermal isomerization step is slightly faster than the isomerization of the analogous unstable *cis*-**4** to stable *trans*-**4** ($t_{1/2} = 8.2$ h, at rt).

**^{1}H NMR Measurements of Molecular Motor 5.** The isomerization steps during the rotation process of motor **5** were studied in more detail by ^{1}H NMR spectroscopy. Solutions[18] of pure stable *trans*-**5** and stable *cis*-**5** isomers in dichloromethane-$d_2$ were both irradiated with UV light ($\lambda \geq 365$ nm) at −40 °C.

Distinctive features in the ^{1}H NMR spectrum of stable *trans*-**5** (Figure 4a) are absorptions of the aliphatic protons at 2.75 ppm (d, H$_b$), 3.48 ppm (dd, H$_c$), and 4.21 ppm (d, H$_a$). Upon irradiation of the solution of stable *trans*-**5**, the doublet absorption at 2.75 ppm is shifted downfield and the double doublet at 3.50 is shifted upfield so these absorptions appear together at 3.23−3.45 ppm (m, H$_b$ + H$_c$) (Figure 4b). Comparison with data obtained for motor **4** confirms that the unstable *cis* isomer is formed. In addition, no residual *trans* isomer is left in the solution, so the photochemical isomerization step gives a conversion >95% toward unstable *cis*-**5**. A subsequent thermal helix inversion (at rt, overnight) produced stable *cis*-**5**, but also a considerable amount of stable *trans*-**5** (*cis*/*trans* ratio 43:57) was observed (Figure 4c). In contrast, performing the thermal step at 40 °C for 2 h gave a different ratio of stable *cis* and stable *trans* isomers (*cis*/*trans* ratio 77:23) (Figure 4d). To confirm these results, the stable *trans* to stable *cis* isomerization was examined in a different solvent by ^{1}H NMR measurements. After the
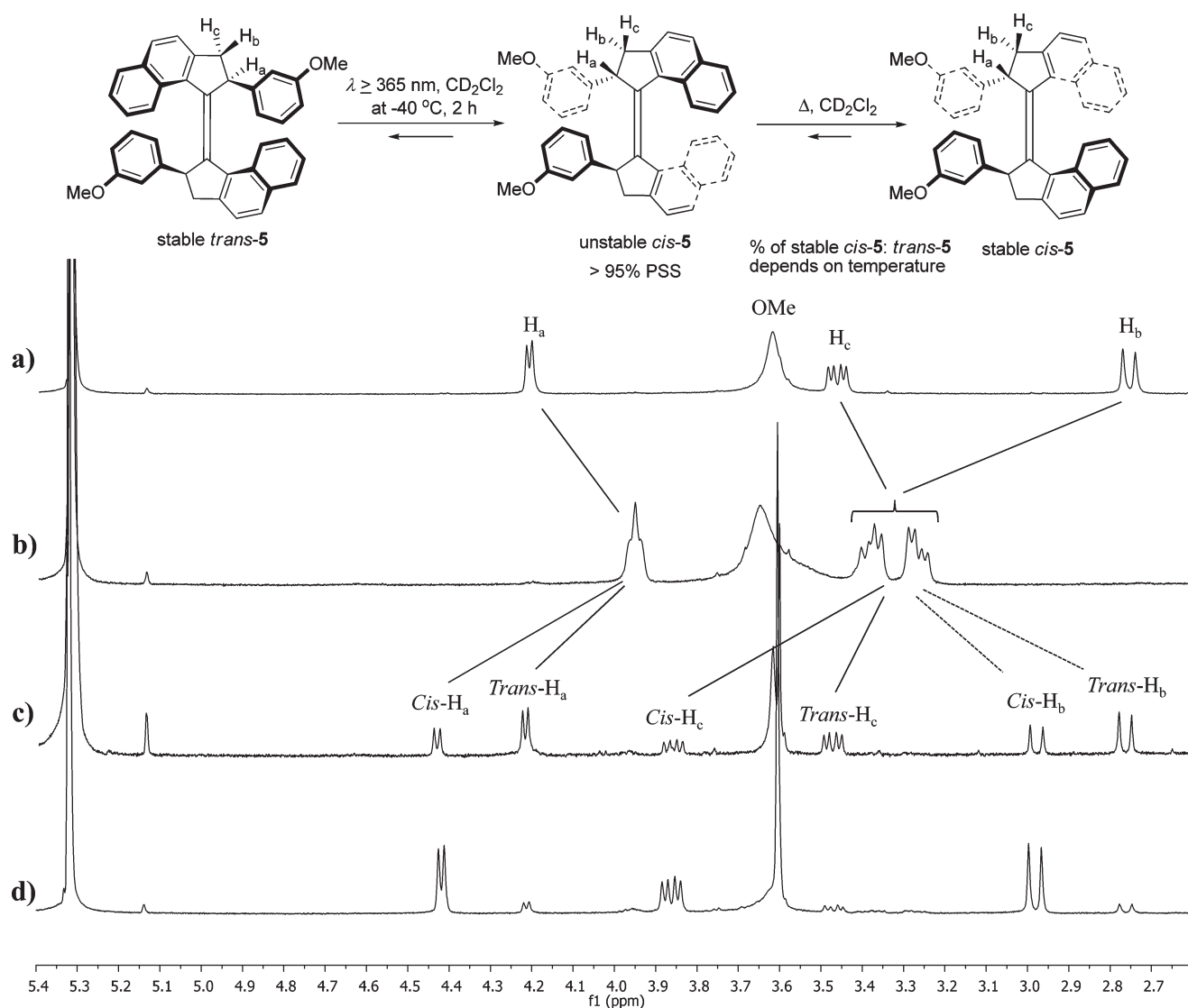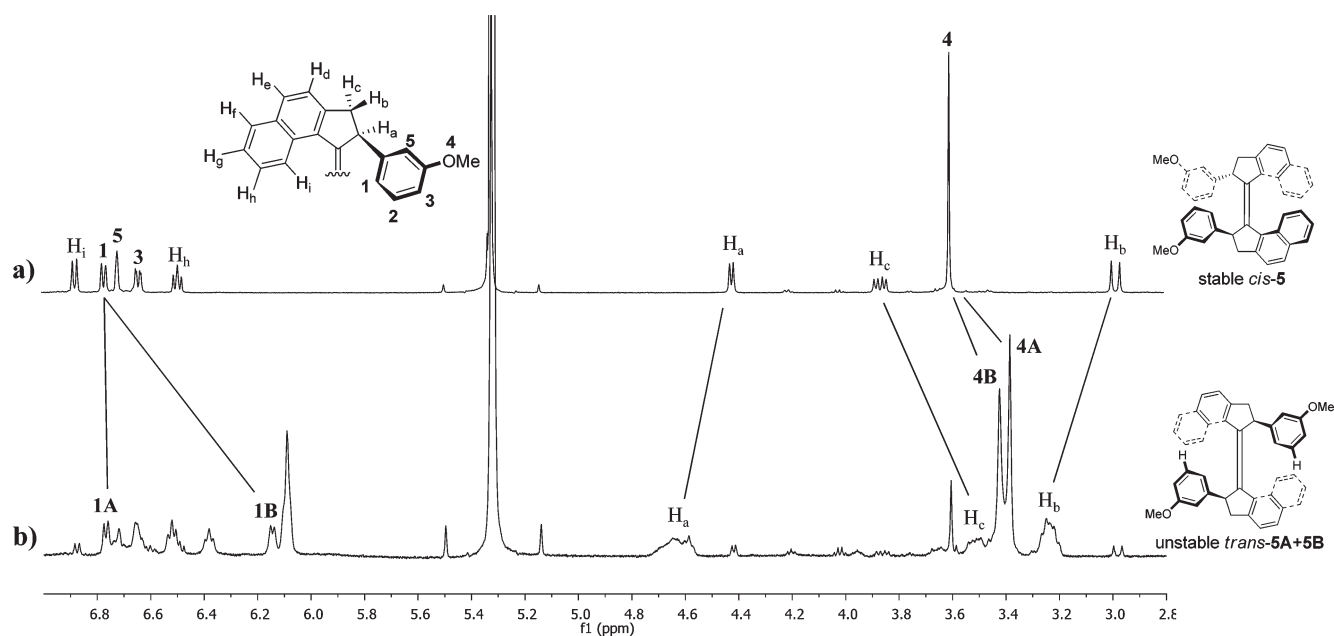
**Figure 4.** $^1$H NMR spectra (500 MHz) of 5 in CD$_2$Cl$_2$: (a) stable *trans*-5; (b) unstable *cis*-5 obtained by photochemical isomerization ($\lambda \geq 365$ nm) from stable *trans*-5; (c) stable *cis*-5 obtained by thermal helix inversion from unstable *cis*-5 at rt; (d) stable *cis*-5 obtained by thermal helix inversion from unstable *cis*-5 at 40 °C (all spectra were recorded at −40 °C).

photochemical isomerization step of stable *trans*-5 in toluene-$d_8$ (unstable *cis* > 95%), $^1$H NMR spectra were recorded first at rt, and it was found that under these conditions the unstable *cis*-5 undergoes a forward isomerization to stable *cis*-5 as well as a competing backward isomerization to the stable *trans* isomer (stable *cis*/stable *trans* ratio, 63:37). When unstable *cis*-5 (>95%) in toluene-$d_8$ was used at higher temperatures, it was observed that the thermal isomerization process of unstable *cis*-5 at 70 °C gave a considerable amount of stable *cis*-5 (*cis*/*trans* ratio, 76:24) (see Figure S2, Supporting Information). Formation of the stable *trans* isomer means that isomerization from unstable *cis*-5 to stable *cis*-5 is not a completely unidirectional rotation process (reversible). Even in a different solvent and at different temperatures, the unstable *cis* isomer still shows competition between forward rotation to stable *cis*-5 and backward rotation to stable *trans*-5. This behavior of molecular motors showing a competing backward thermal helix inversion was also observed for some other systems,[20] and the consequences for the unidirectional nature of the overall motor function were expressed in a mathematical model.[21] The present system shows similar behavior and the competing backward thermal helix inversion is the consequence of the replacement of the substituent at the stereogenic center and the relatively high barrier for thermal isomerization. From these results, it is evident that the ratio of stable *cis* and *trans* isomers depends on the temperature at which the thermal helix inversion process takes place.[21] Nevertheless, there is a large preference for the forward direction, which allows a major unidirectional rotary motion.

The next step in the rotary cycle was performed with stable *cis*-5; two of the three aliphatic protons of stable *cis*-5 (CD$_2$Cl$_2$, −40 °C) are found at 2.95 ppm (d, H$_b$) and at 3.85 ppm (dd, H$_c$) as shown in Figure 5a. Irradiation of stable *cis*-5 resulted in a downfield shift of the absorption of H$_b$ from 2.95 to 3.25 ppm and upfield shift of the absorption of H$_c$ from 3.85 to 3.50 ppm (Figure 5b). Formation of the unstable *trans* isomer was also confirmed by comparison with data obtained for motor **4**. Moreover, in this spectrum of unstable *trans*-5, the decrease in the rate of rotation of the rotor part (*m*-methoxyphenyl) is clearly visible.

**Figure 5.** ^{1}H NMR spectra (500 MHz) in CD$_2$Cl$_2$ at −40 °C of (a) stable *cis*-**5** and (b) unstable *trans*-**5** after irradiation ($\lambda \geq 365$ nm) showing the distinct absorption for the methoxy group (**A** and **B**).

**Scheme 4. Rotamers A and B of Unstable *trans*-5**
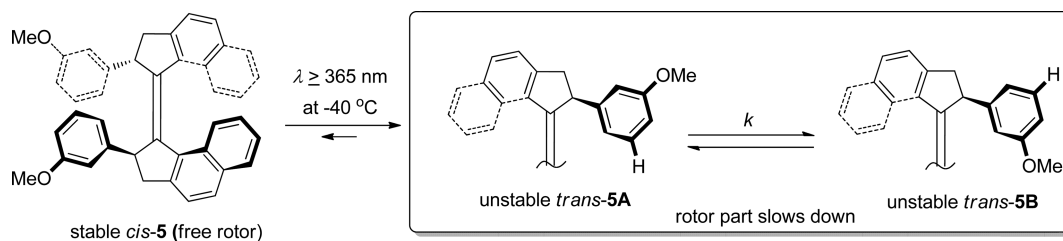


For all three other isomers (stable *trans*, stable *cis*, and unstable *cis*), the singlet of the methoxy group appears at 3.6 ppm (s, 3H). However, in the spectrum of unstable *trans*-**5**, this absorption appears as two singlets at around 3.40−3.45 ppm. This implies that the rotation of the rotor moiety is slow on the NMR time scale, which in turn implies that ^{1}H NMR spectroscopy can be used to distinguish between two different relative positions (**A** and **B**) of the methoxy substituent in this isomer and to establish the barrier of rotation by temperature dependent ^{1}H NMR measurements (Scheme 4).

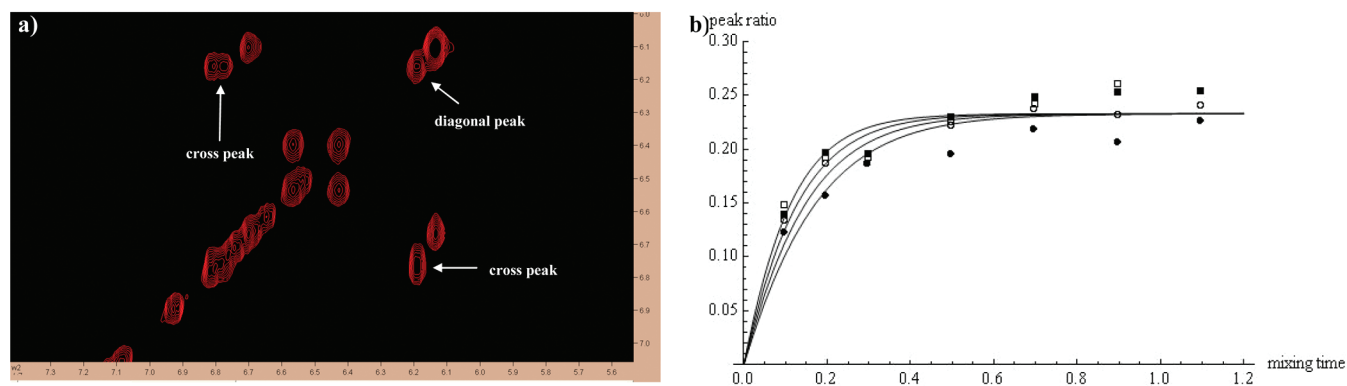In the ^{1}H NMR spectrum of unstable *trans*-**5** at −40 °C,[22] some residual stable *cis*-**5** is still visible after irradiation, and the PSS was calculated to consist of 75% of unstable *trans*-**5** and 25% of stable *cis*-**5** (see Figure S5b, Supporting Information). The ^{1}H NMR spectrum of the sample after heating (20 °C for 20 min) revealed that all of the absorptions of unstable *trans*-**5** were replaced by the absorptions expected from stable *trans*-**5**, exemplified by the shift of one of the protons in the aliphatic region from 3.25 to 2.75 ppm (see Figure S5c, Supporting Information). These ^{1}H NMR data indicated that the thermal isomerization of unstable *trans*-**5** quantitatively gave stable *cis*-**5**, and as a consequence, a ratio of stable *trans*-**5** to stable *cis*-**5** of 75:25 was found. This means that this thermal isomerization from stable *cis*-**5** to stable *trans*-**5** is a unidirectional process. These photochemical

and thermal isomerization steps (from stable *cis* to stable *trans* isomers) result in a 180° rotation of the upper half of the molecule with respect to the other half (as for **4** in Scheme 3).

**2D-EXSY Measurements for the Rotor Functions of the Molecular Motor.** Initial studies of the rate of rotation of the rotor moiety were carried out with the unstable *trans* isomer, generated by photoisomerization of stable *cis*-**5**. However, because of the high activation barrier of the rotor, coalescence studies using ^{1}H NMR are not suitable to determine the rate of exchange (rate of rotation, *k*) of the anisole group.[23] Because the half-life of unstable *trans*-**5** to stable *trans*-**5** is very short at rt, thermal isomerization occurs before the rotation of the rotor unit can be examined. Therefore, the exchange of the methoxy group of the *m*-methoxyphenyl substituent is only visible on the NMR time scale at low temperature. 2D-EXSY spectra of unstable *trans*-**5** were obtained at different temperatures of −50, −45, −40, and −35 °C, with different mixing times of 0.1, 0.2, 0.3, 0.5, 0.7, 0.9, and 1.1 s in dichloromethane-*d$_2$*. Figure 6a shows a 2D-EXSY spectrum (see general remarks). The presence of exchange cross peaks immediately showed that, as expected, the rotation of the rotor around the biaryl bond connecting the rotor moiety to the motor in the unstable *trans* isomer is hindered.[24,25]

Unstable *trans*-**5** can be approached as an asymmetrical two-site exchange system between a proton and a methoxy at the *m*-anisole

**Figure 6.** (a) 2D-EXSY spectrum of unstable *trans*-**5** (500 MHz, CD$_2$Cl$_2$) at −40 °C (mixing time 0.2 s). (b) Graph showing the relation between mixing time and the ratio between cross (proton 1A) and diagonal peaks (proton 1B) for unstable *trans*-**5** at −35 °C (top line, empty squares), −40 °C (second line, filled squares), −45 °C (third line, empty circles), and −50 °C (bottom line, filled circles).

moiety (Scheme 4). By rotating around a single bond that connects the rotor (*m*-anisole) to the motor, the methoxy group exchanges its position with that of the proton on the other side of the phenyl moiety. One of these conformations is higher in energy than the other because of steric interaction between the methoxy group and the naphthalene moiety. This means the conformations will not be equally populated and, therefore, the ratio of cross peaks and diagonal peaks will not converge to 1.

This can be resolved by adding an extra parameter $p$ to the equation (eq 1; see the Experimental Section, general remarks) when fitting a line to the data points in Figure 6b. Parameter $p$ represents the population of one of the exchange sites, the population of the other site being $1 − p$. In case of symmetrical exchange, $p$ is 0.5. Because the ratio of cross peaks and diagonal peaks is directly proportional to the population of the exchange sites, the peak ratio will approach to $p/(1 − p)$. In this case this is 0.23, as can be observed in Figure 6b, where peak ratios are plotted versus mixing times. From the peak ratio, the extra parameter $p$ can be calculated for the rotor part of molecular motor **5** to be 0.19.[26]

From this graph, the Gibbs free energy of activation ($\Delta^{\ddagger}G°$) for the rotation of the rotor was calculated to be 11.6 kJ·mol$^{-1}$. Using the Eyring equation, the rate of exchange (rate of rotation; $k$) has been calculated to be 8.1 × 10$^9$ s$^{-1}$ at 20 °C. The $^1$H NMR spectra of the other three isomers (stable *trans*, unstable *cis* ,and stable *cis*) show that the rotation of the rotor part is unhindered (free rotation around the single bond). This means that motor **5** behaves as a coupled rotary system. By simple isomerization from stable *cis*-**5** to unstable *trans*-**5**, the rotation rate of the bidirectional rotor can be altered significantly. Thermal helix inversion to stable *trans*-**5** or photoisomerization to stable *cis*-**5** returns the rotor to its original, unhindered state. Although this molecular motor **5** is not as sophisticated as the "second-generation" molecular gearbox **3**, this motor can be used as a rotation-on-rotation–off switching system by photoisomerization from stable *cis*-**5** to unstable *trans*-**5** and back again (Scheme 4). Due to its simple design, this will be a very useful function in more advanced coupled rotary systems.

## CONCLUSIONS

In summary, a new synthetic route toward functionalized first-generation molecular motors has been developed, reducing the number of synthetic steps from seven to three. A number of different aryl-substituted ketone precursors for first-generation motors are readily accessible.

First-generation molecular motors with phenyl and *m*-anisole groups at the stereogenic centers have been synthesized, and the dynamic behavior of these new first-generation molecular motors has been studied in detail. Even though the UV−vis studies confirm the four-step rotary cycle and $^1$H NMR studies show that conversion for both photochemical steps is near 100%, the thermal step from unstable *cis* to stable *cis* in the rotary cycle is not completely unidirectional for motor **5**. A major goal of this study was to examine how the rotary motion of an appending rotor unit can be controlled by the light-driven motor function. It has been demonstrated that the rate of rotation of the *m*-anisole rotor embedded in these molecular motors can be controlled using light and heat as external triggers. The rotation properties of the *m*-anisole moiety have been studied in detail using $^1$H NMR and 2D-EXSY spectroscopy. The results show that the rotation of the *m*-anisole moiety in **5** is unhindered in the stable *trans*, unstable *cis*, and stable *cis* isomers but hindered in the unstable *trans* isomer. Therefore, the system can be used as a light-switch between a state of free rotor rotation and a state of hindered (slow) rotor rotation. Our findings on the control of the speed of rotation of the rotors will be useful in the design of more advanced molecular motors, in particular to control coupled motion.

## EXPERIMENTAL SECTION

**General Remarks.** All reactions were carried out in oven-dried glassware under a nitrogen atmosphere. Solvents were reagent grade, distilled and dried before use according to standard procedures. Other commercially available reagents were used without purification. Irradiation experiments were performed using an ENB-280C/FE lamp ($\lambda \geq$ 365 nm). Samples irradiated for $^1$H NMR spectroscopic analysis were placed 2−3 cm from the lamp. Photostationary states were determined by monitoring composition changes into time by taking UV−vis spectra or $^1$H NMR spectra at distinct intervals until no additional changes were observed. Kinetic analysis of the thermal isomerization steps was performed by UV−vis spectroscopy. A high-pass filter was mounted in front of the UV light source to cut off all light with a wavelength below 380 nm to minimize photochemical isomerization occurring upon data recording. Changes in UV−vis absorptions were measured at different temperatures: for unstable *trans*- to stable *trans*-isomers in DCM at −20, −15, −12, −10, and −5 °C and for unstable *cis*- to stable *cis*-isomers in DCE at 30, 40, 50, and 60 °C. From the obtained data the rate constants ($k$) were obtained and an Eyring plot was made for both thermal steps

and $\Delta^{\ddagger}H^{\circ}$, $\Delta^{\ddagger}S^{\circ}$, $\Delta^{\ddagger}G$, and $t_{1/2}$ (at 20 °C) of both *cis-* and *trans-* isomerizations were calculated from these data.

For the 2D-EXSY measurements, signals on the diagonal line are referred to as "diagonal peaks"; these are the two-dimensional depiction of the $^1$H NMR spectrum of the compound. Signals deviating from this line are called "cross peaks". Every cross peak can be connected to two corresponding diagonal peaks and one other cross peak, and this set of absorptions is indicative of an exchange process. By assigning and integrating the cross peaks and corresponding diagonal peaks, information about exchange processes in the compound **5** can be obtained (for details, see ref 25).

A cross peak and one of its corresponding diagonal peaks were then selected from the 2D spectrum, in this case, protons 1A and 1B (Figure 6a); for accuracy, it is important that there is the least possible amount of overlap with any other absorption. For these peaks (protons 1A and **1B**), the integrals are calculated and divided by each other to give the peak ratio ($p/(1 - p)$).

First, the ratio of diagonal peaks and their corresponding cross peaks in the 2D-EXSY spectrum were plotted against the different mixing times ($\tau_{mix}$) for the different temperatures (Figure 6b). Subsequently, a curve was fitted for each different temperature using the following function:

$$f(T, \tau_{mix}) = p(1 - \exp[k_0 \cdot \exp((-\Delta^{\ddagger}G/R)((1/T)-(1/T_0))\tau_{mix}])/1$$
$$- p(1 - \exp[k_0 \exp((-\Delta^{\ddagger}G/R)((1/T) - (1/T_0))\tau_{mix}]) \quad (1)$$

In this function, $T$ and $\tau_{mix}$ represent the different temperatures and mixing times, respectively. $R$ is the gas constant ($8.3 \text{ J} \cdot \text{K}^{-1} \cdot \text{mol}^{-1}$). $p$ (population), $\Delta^{\ddagger}G$ (Gibbs free energy of activation at temperature $T_0$), and $k_0$ were used as fitting parameters. Subsequently, the rate of exchange ($k$) was calculated using the Eyring equation. The notebook in which the 2D-EXSY calculations were performed was developed by Dr. E. Otten and Dr. R. Scheek, based on the literature.[27]

### Synthesis of the α-Aryl Ketones 6 and Molecular Motors 4 and 5.

*2,3-Dihydro-1H-cyclopenta[a]naphthalen-1-one (**7**).* A solution of β-chloropropionyl chloride (7.5 mL, 78 mmol) and naphthalene (10 g, 78 mmol) in 25 mL of carbon disulfide (CS$_2$) under a nitrogen atmosphere was added over 45 min to anhydrous AlCl$_3$ (13 g, 94 mmol) in CS$_2$ (100 mL). After 4 h of stirring at room temperature, the carbon disulfide was removed under reduced pressure to provide a crude oil. To the residual oil 50 mL of concentrated H$_2$SO$_4$ was added, and the mixture was heated at 90 °C for 40 min. After being cooled to room temperature, the mixture was poured onto 200 g of crushed ice and the reaction mixture was extracted with ether. The combined organic layers were washed with water, saturated aq NaHCO$_3$, and brine, dried over Na$_2$SO$_4$, and filtered, and the volatiles were removed in vacuo. The crude material was purified by flash column chromatography (SiO$_2$, pentane/EtOAc; 95:5, $R_f = 0.64$) yielding **7** (11 g, 58 mmol, 74%) as a white solid: mp 105.0−105.3 °C; $^1$H NMR (400 MHz, CDCl$_3$) δ 2.69 (t, J = 5.3 Hz, 2H), 3.07 (t, J = 5.3 Hz, 2H), 7.37 (d, J = 8.2 Hz, 1H), 7.50 (t, J = 7.0 Hz, 1H), 7.62 (t, J = 8.2 Hz, 1H), 7.81 (d, J = 8.2 Hz, 1H), 7.91 (d, J = 8.5 Hz, 1H), 9.11 (d, J = 8.2 Hz, 1H); $^{13}$C NMR (101 MHz, CDCl$_3$) δ 26.0 (CH$_2$), 36.7 (CH$_2$), 123.7 (CH), 123.8 (CH), 126.4 (CH), 127.9 (CH), 128.6 (CH), 129.2 (C), 130.7 (C), 132.4 (C), 135.4 (CH), 158.2 (C), 207.2 (C); HRMS (ESI) *m/z* calcd. for C$_{13}$H$_{10}$O 182.0732, found 182.0735.

*General Procedure A for α-Arylation Reaction: 2-(3,5-Dimethylphenyl)-2,3-dihydro-1H-cyclopenta[a]naphthalen-1-one (**6.1**).* Pd(OAc)$_2$ (0.22 g, 0.96 mmol), t-BuONa (0.46 g, 4.8 mmol), and 2-dicyclohexylphosphino-2′,4′,6′-triisopropylbiphenyl (0.92 g, 1.9 mmol) were dissolved in toluene (5 mL) under a nitrogen atmosphere. A solution of ketone **7** (0.42 g, 2.30 mmol) and 1-iodo-3,5-dimethylbenzene (0.33 mL, 1.9 mmol) in toluene (5 mL) was added. The mixture was stirred and heated at reflux overnight. After the mixture was cooled to room temperature, water (25 mL) was added,

and the mixture was extracted with diethyl ether (3 × 25 mL), washed with water (25 mL), dried (Na$_2$SO$_4$), filtered, and concentrated in vacuo. The crude product was purified by flash column chromatography (SiO$_2$, pentane: EtOAc; 9: 1, $R_f = 0.58$). Ketone **6.1** was obtained as a brown powder (0.32 g, 1.18 mmol, 62%): $^1$H NMR (400 MHz, CDCl$_3$) δ 2.28 (s, 6H), 3.34 (dd, J = 15.4, 5.4 Hz, 1H), 3.70−3.80 (m, 1H), 3.91 (dd, J = 9.7, 4.8 Hz, 1H), 6.83 (s, 2H), 6.90 (s, 1H), 7.54−7.61 (m, 2H), 7.64−7.72 (m, 1H), 7.92 (d, J = 8.4 Hz, 1H), 8.10 (d, J = 8.5 Hz, 1H), 9.16 (d, J = 8.7 Hz, 1H); $^{13}$C NMR (101 MHz, CDCl$_3$) δ 21.3 (CH), 36.3 (CH$_2$), 53.8 (CH$_3$), 123.8 (CH), 124.2 (CH), 125.6 (CH), 126.7 (CH), 128.1 (CH), 128.7 (CH), 129.0 (CH), 129.7 (C), 130.2 (C), 132.9 (C), 136.1 (CH), 138.4 (C), 139.9 (C), 157.2 (C), 206.7 (C); HRMS (ESI) *m/z* calcd for C$_{21}$H$_{18}$O 286.3670, found 286.3633.

*2-(2,6-Dimethylphenyl)-2,3-dihydro-1H-cyclopenta[a]naphthalen-1-one (**6.2**).* Ketone **6.2** was prepared via general procedure A from ketone **7** (117 mg, 0.65 mmol) and 1-iodo-2,6-dimethylbenzene (100 mg, 0.43 mmol) using Pd(OAc)$_2$ (48 mg, 0.22 mmol), t-BuONa (120 mg, 1.29 mmol), and 2-dicyclohexylphosphino-2′,4′,6′-triisopropylbiphenyl (210 mg, 0.43 mmol). The crude product was purified using flash column chromatography (SiO$_2$, pentane/EtOAc 9:1, $R_f = 0.55$). Ketone **6.2** was obtained as a pale yellow powder (82 mg, 0.29 mmol, 67%): $^1$H NMR (400 MHz, CDCl$_3$) δ 1.91 (s, 3H), 2.48 (s, 3H), 3.25 (dd, J = 17.5, 4.5 Hz, 1H), 3.74 (dd, J = 17.9, 8.1 Hz, 1H), 4.38 (dd, J = 8.0, 4.8 Hz, 1H), 7.00 (t, J = 4.5 Hz, 1H), 7.10 (d, J = 4.7 Hz, 2H), 7.54−7.63 (m, 2H), 7.70 (t, J = 7.6 Hz, 1H), 7.94 (d, J = 8.2 Hz, 1H), 8.11 (d, J = 8.4 Hz, 1H), 9.24 (d, J = 8.4 Hz, 1H); $^{13}$C NMR (101 MHz, CDCl$_3$) δ 21.3 (CH), 34.2 (CH$_2$), 50.4 (CH$_3$), 123.8 (CH), 124.1 (CH), 126.7 (CH), 126.9 (CH), 128.12 (CH), 128.14 (CH), 128.9 (CH), 129.4 (CH), 130.8 (C), 132.9 (C), 135.8 (CH), 136.4 (C), 137.8 (C), 155.5 (C), 207.0 (C); HRMS (ESI) *m/z* calcd for C$_{21}$H$_{19}$O 287.1430, found 287.1439.

*2-Phenyl-2,3-dihydro-1H-cyclopenta[a]naphthalen-1-one (**6.3**).* Ketone **6.3** was prepared via general procedure A from ketone **7** (0.13 g, 0.74 mmol) and iodobenzene (0.1 g, 0.49 mmol) using Pd(OAc)$_2$ (55 mg, 0.25 mmol), t-BuONa (0.14 g, 1.47 mmol), and 2-dicyclohexylphosphino-2′,4′,6′-triisopropylbiphenyl (0.23 g, 0.49 mmol). The crude product was purified using flash column chromatography (SiO$_2$, pentane/EtOAc; 85:15, $R_f = 0.54$). Ketone **6.3** was obtained as a brown powder (88.5 mg, 0.34 mmol, 70%): $^1$H NMR (400 MHz, CDCl$_3$) δ 3.36 (dd, J = 17.9, 3.4 Hz, 1H), 3.75 (dd, J = 17.9, 7.9 Hz, 1H), 3.99 (dd, J = 7.9, 3.4 Hz, 1H), 7.24−7.30 (m, 3H), 7.33−7.38 (m, 2H), 7.55−7.61 (m, 2H), 7.69 (t, J = 7.6 Hz, 1H), 7.93 (d, J = 8.1 Hz, 1H), 8.10 (d, J = 8.4 Hz, 1H), 9.19 (d, J = 8.3 Hz, 1H); $^{13}$C NMR (101 MHz, CDCl$_3$) δ 36.2 (CH$_2$), 53.9 (CH), 123.8 (CH), 124.1 (CH), 126.8 (CH), 127.0 (CH), 127.9 (CH), 128.2 (CH), 128.9 (CH), 129.1 (CH), 129.7 (C), 130.2 (C), 132.9 (C), 136.2 (CH), 140.0 (C), 157.1 (C), 206.4 (C); HRMS (ESI) *m/z* calcd for C$_{19}$H$_{14}$O 258.1045, found 258.1041.

*2-(3-Methoxyphenyl)-2,3-dihydro-1H-cyclopenta[a]naphthalen-1-one (**6.4**).* Ketone **6.4** was prepared via general procedure A from ketone **7** (0.57 g, 3.1 mmol) and 1-iodo-3-methoxybenzene (0.61 g, 2.6 mmol) using Pd(OAc)$_2$ (0.29 g, 1.3 mmol), t-BuONa (0.62 g, 6.4 mmol), and 2-dicyclohexylphosphino-2′,4′,6′-triisopropylbiphenyl (1.2 g, 2.6 mmol). The crude product was purified using flash column chromatography (SiO$_2$, pentane/EtOAc; 4:1, $R_f = 0.45$). Ketone **6.4** was obtained as a yellow oil (0.31 g, 1.09 mmol, 35%): $^1$H NMR (400 MHz, CDCl$_3$) δ 3.36 (dd, J = 17.8, 3.4 Hz, 1H), 3.72−3.81 (m, 4H), 3.97 (dd, J = 7.9, 3.4 Hz, 1H), 6.77−6.85 (m, 3H), 7.21−7.29 (m, 1H), 7.55−7.60 (m, 2H), 7.68 (ddd, J = 8.3, 7.0, 1.3 Hz, 1H), 7.92 (d, J = 8.1 Hz, 1H), 8.11 (d, J = 8.4 Hz, 1H), 9.15 (d, J = 8.4 Hz, 1H); $^{13}$C NMR (101 MHz, CDCl$_3$) δ 36.1 (CH$_2$), 53.8 (CH), 55.2 (CH$_3$), 112.3 (CH), 113.8 (CH), 120.1 (CH), 123.7 (CH), 124.1 (CH), 126.8 (CH), 128.1 (CH), 129.1 (CH), 129.7 (C), 129.8 (CH), 130.2 (C), 132.9 (C), 136.2 (CH), 141.5 (C), 157.1 (C), 159.9 (C), 206.2 (C); HRMS (ESI) *m/z* calcd for C$_{20}$H$_{16}$O$_2$ 289.1223, found 289.1208 (M + H$^+$).

*2-(4-Methoxyphenyl)-2,3-dihydro-1H-cyclopenta[a]naphthalen-1-one (6.5).* Ketone **6.5** was prepared via general procedure A from ketone **7** (93 mg, 0.51 mmol) and 1-iodo-3-methoxybenzene (100 mg, 0.43 mmol) using Pd(OAc)$_2$ (47.9 mg, 0.21 mmol), *t*-BuONa (103 mg, 1.07 mmol), and 2-dicyclohexylphosphino-2′,4′,6′-triisopropylbiphenyl (204 mg, 0.43 mmol). The crude product was purified using flash column chromatography (SiO$_2$, pentane/EtOAc; 4:1, $R_f$ = 0.47). Ketone **6.5** was obtained as a pale yellow oil (16.1 mg, 0.056 mmol, 13%): $^1$H NMR (400 MHz, CDCl$_3$) δ 3.33 (dd, J = 17.8, 3.4 Hz, 1H), 3.76 (dd, J = 11.9, 6.0 Hz, 1H), 3.79 (s, 3H), 3.95 (dd, J = 7.9, 3.5 Hz, 1H), 6.87 (d, J = 8.7 Hz, 2H), 7.16 (d, J = 8.7 Hz, 2H), 7.56−7.61 (m, 2H), 7.67 (t, J = 7.7 Hz, 1H), 7.92 (d, J = 8.5 Hz, 1H), 8.10 (d, J = 8.4 Hz, 1H), 9.14 (d, J = 8.3 Hz, 1H); $^{13}$C NMR (101 MHz, CDCl$_3$) δ 36.2 (CH$_2$), 53.0 (CH), 55.3 (CH$_3$), 114.3 (CH), 123.8 (CH), 124.1 (CH), 126.7 (CH), 128.1 (CH), 128.8 (CH), 129.0 (CH), 129.7 (C), 130.1 (C), 132.0 (C), 132.9 (C), 136.1 (CH), 156.9 (C), 158.6 (C), 206.7 (C); HRMS (ESI) *m/z* calcd for C$_{20}$H$_{16}$O$_2$ 289.1223, found 289.1233 (M + H$^+$).

*2-(3-((tert-Butyldiphenylsilyloxy)methyl)phenyl)-2,3-dihydro-1H-cyclopenta[a]naphthalen-1-one (6.7).* Ketone **6.7** was prepared via general procedure A from ketone **7** (0.71 g, 3.93 mmol) and *tert*-butyl(3-iodobenzyloxy)diphenylsilane (1.53 g, 3.25 mmol) using Pd-(OAc)$_2$ (0.36 g, 1.62 mmol), *t*-BuONa (0.78 g, 8.13 mmol), and 2-dicyclohexylphosphino-2′,4′,6′-triisopropylbiphenyl (1.55 g, 3.25 mmol). The crude product was purified using flash column chromatography (SiO$_2$, pentane/EtOAc; 95:5, $R_f$ = 0.42). Ketone **6.7** was obtained as a yellow oil (1.09 g, 2.07 mmol, 64%): $^1$H NMR (400 MHz, CDCl$_3$) δ 1.07 (s, 9H), 3.36 (dd, J = 17.9, 3.2 Hz, 1H), 3.77 (dd, J = 17.9, 7.9 Hz, 1H), 4.01 (dd, J = 7.9, 3.2 Hz, 1H), 4.79 (s, 2H), 7.19 (s, 1H), 7.32−7.46 (m, 10H), 7.65−7.71 (m, 4H), 7.77 (d, J = 7.9 Hz, 2H), 7.95 (d, J = 8.1 Hz, 1H), 8.12 (d, J = 8.4 Hz, 1H), 9.20 (d, J = 8.4 Hz, 1H); $^{13}$C NMR (101 MHz, CDCl$_3$) δ 19.20 (C), 26.73 (CH$_3$), 36.22 (CH$_2$), 53.73 (CH), 65.27 (CH$_2$), 123.70 (CH), 124.08 (CH), 124.53 (CH), 124.92 (CH), 126.58 (CH), 126.68 (CH), 127.62 (CH), 127.64 (CH), 128.09 (CH), 128.69 (CH), 129.00 (CH), 129.56 (CH), 129.59 (CH), 129.71 (C), 130.14 (C), 132.86 (C), 133.36 (C), 134.75 (CH), 135.18 (C), 135.48 (CH), 136.11 (CH), 139.94 (C), 141.63 (C), 157.16 (C), 206.42 (C), four (CH) absorptions of aromatic protons were not observed (overlapping signal); HRMS (ESI) *m/z* calcd for C$_{36}$H$_{34}$O$_2$Si 527.2401, found 527.2425 (M + H$^+$).

*General Procedure B for the McMurry Coupling Reaction: 2,2′-Bis(3-phenyl)-2,2′,3,3′-tetrahydro-1,1′-bi(cyclopenta[a]naphthalenylidene) (4).* TiCl$_4$ (0.17 mL, 1.5 mmol) was added dropwise to a stirred suspension of zinc powder (203 mg, 3.1 mmol) in THF (10 mL) at room temperature. The mixture was heated at reflux for 2 h in an oil bath. Ketone **6.3** (200 mg, 0.8 mmol) in THF (5 mL) was added, and the mixture was stirred overnight at reflux. The mixture was then cooled, added to 25 mL of a saturated aqueous solution of NH$_4$Cl, and extracted with Et$_2$O (3 × 20 mL). The combined organic layers were washed with brine (2 × 20 mL), dried over Na$_2$SO$_4$, filtered, and concentrated in vacuo. Alkene **4** was obtained (31 mg, 0.064 mmol, 16%) as a mixture of *trans*- and *cis*-isomers in approximately a 2:1 ratio. A mixture of *trans*-**4** and *cis*-**4** was purified by flash chromatography (silica gel; heptane/toluene; 99:1 to 95:5, $R_f$-*trans* = 0.21, $R_f$-*cis* = 0.14) to give the *trans*-**4** (22 mg, 0.045 mmol, 11%) and *cis*-**5** (9 mg, 0.019 mmol, 5%).

*trans*-**4** (pale yellow solid): $^1$H NMR (400 MHz, CDCl$_3$) δ 2.79 (d, J = 14.9 Hz, 1H), 3.51 (dd, J = 14.9, 6.6 Hz, 1H), 4.29 (d, J = 6.5 Hz, 1H), 6.87 (t, J = 8.1 Hz, 1H), 7.11−7.15 (m, 2H), 7.16−7.21 (m, 3H), 7.27 (d, J = 8.8 Hz, 1H), 7.32−7.37 (m, 1H), 7.73 (d, J = 8.1 Hz, 2H), 7.84 (d, J = 8.0 Hz, 1H); $^{13}$C NMR (101 MHz, CDCl$_3$) δ 43.4 (CH$_2$), 54.1 (CH), 123.7 (CH), 124.9 (CH), 125.4 (CH), 125.8 (CH), 127.8 (CH), 128.09 (CH), 128.13 (CH), 128.2 (CH), 128.7 (CH), 129.0 (C), 133.0 (C), 139.4 (C), 140.3 (C), 140.8 (C), 145.4 (C); HRMS (ESI) *m/z* calcd for C$_{38}$H$_{28}$ 484.2191, found 484.2197.

*cis*-**4** (yellow solid): $^1$H NMR (400 MHz, CDCl$_3$) δ 2.97 (d, J = 15.6 Hz, 1H), 3.86 (dd, J = 15.6, 7.3 Hz, 1H), 4.51 (d, J = 7.1 Hz, 1H), 6.48 (t, J = 7.6 Hz, 1H), 6.84 (d, J = 8.4 Hz, 1H), 7.04 (t, J = 7.5 Hz, 1H), 7.13−7.21 (m, 5H), 7.38 (d, J = 8.2 Hz, 1H), 7.68−7.75 (m, 2H); $^{13}$C NMR (101 MHz, CDCl$_3$) δ 42.4 (CH$_2$), 52.9 (CH), 123.2 (CH), 124.4 (CH), 124.5 (CH), 126.1 (CH), 126.7 (CH), 127.2 (CH), 127.9 (CH), 128.5 (CH), 129.1 (C), 129.3 (CH), 132.4 (C), 138.1 (C), 139.0 (C), 144.0 (C), 145.7 (C); HRMS (ESI) *m/z* calcd for C$_{38}$H$_{28}$ 484.2191, found 484.2164.

**2,2′-Bis(3-methoxyphenyl)-2,2′,3,3′-tetrahydro-1,1′-bi-(cyclopenta[a]naphthalenylidene) (5).** Molecular motor **5** was prepared by general procedure B. TiCl$_4$ (0.20 mL, 1.8 mmol) was added dropwise to a stirred suspension of Zn (0.24 g, 3.6 mmol) in THF (10 mL) at room temperature. The mixture was heated at reflux for 2 h in an oil bath. Ketone **6.4** (0.26 g, 0.91 mmol) in THF (5 mL) was added, and the mixture was stirred overnight at reflux. The mixture was then cooled, added to 25 mL of a saturated aqueous solution of NH$_4$Cl, and extracted with Et$_2$O (3 × 20 mL). The combined organic layers were washed with brine (2 × 20 mL), dried over Na$_2$SO$_4$, filtered, and concentrated in vacuo. Alkene **5** was obtained (85 mg, 0.16 mmol, 35%) as a mixture of *trans*- and *cis*-isomers in approximately a 3:2 ratio. A mixture of *trans*-**5** and *cis*-**5** was purified by chromatography (silica gel; pentane/EtOAc; 99.5:0.5 to 99:1, no air pressure, $R_f$-*trans* = 0.62, $R_f$-*cis* = 0.59) to give the *trans*-**5** (50 mg, 0.092 mmol, 21%) and *cis*-**5** (35 mg, 0.064 mmol, 14%).

*trans*-**5** (white solid, appearing as a yellow fluorescent spot on TLC): $^1$H NMR (400 MHz, CDCl$_3$) δ 2.79 (d, J = 14.9 Hz, 1H), 3.50 (dd, J = 14.9, 6.7 Hz, 1H), 3.61 (s, 3H), 4.26 (d, J = 6.5 Hz, 1H), 6.70 (s, 1H), 6.72 (t, J = 7.9 Hz, 2H), 6.92 (t, J = 7.0 Hz, 1H), 7.10 (t, J = 7.8 Hz, 1H), 7.27 (d, J = 8.9 Hz, 1H), 7.35 (t, J = 7.5 Hz, 1H), 7.73 (d, J = 8.2 Hz, 1H), 7.78 (d, J = 8.5 Hz, 1H), 7.83 (d, J = 8.0 Hz, 1H); $^{13}$C NMR (101 MHz, CDCl$_3$) δ 43.3 (CH$_2$), 54.0 (CH), 55.0 (CH$_3$), 111.4 (CH), 113.8 (CH), 120.6 (CH), 123.7 (CH), 124.9 (CH), 125.5 (CH), 127.7 (CH), 128.2 (CH), 128.8 (CH), 129.0 (C), 129.1 (CH), 133.0 (C), 139.4 (C), 140.2 (C), 140.8 (C), 147.1 (C), 159.3 (C); HRMS (ESI) *m/z* calcd for C$_{40}$H$_{33}$O$_2$ 545.2475, found 545.2492.

*cis*-**5** (yellow solid, appearing as a blue fluorescent spot on TLC): $^1$H NMR (400 MHz, CDCl$_3$) δ 2.99 (d, J = 15.7 Hz, 1H), 3.63 (s, 3H), 3.86 (dd, J = 15.4, 7.2 Hz, 1H), 4.50 (d, J = 7.2 Hz, 1H), 6.47 (t, J = 7.0 Hz, 1H), 6.68 (dd, J = 8.2, 1.8 Hz, 1H), 6.77 (s, 1H), 6.80 (dd, J = 15.1, 8.5 Hz, 2H), 7.02 (t, J = 7.0 Hz, 1H), 7.09 (t, J = 7.8 Hz, 1H), 7.38 (d, J = 8.1 Hz, 1H), 7.68 (d, J = 8.2 Hz, 1H), 7.72 (d, J = 8.2 Hz, 1H); $^{13}$C NMR (101 MHz, CDCl$_3$) δ 42.4 (CH$_2$), 53.0 (CH), 55.0 (CH$_3$), 111.3 (CH), 113.2 (CH), 119.7 (CH), 123.1 (CH), 124.4 (CH), 124.6 (CH), 126.6 (CH), 127.8 (CH), 129.1 (C), 129.3 (CH), 129.4 (CH), 132.4 (C), 138.1 (C), 138.9 (C), 144.0 (C), 147.3 (C), 159.6 (C); HRMS (ESI) *m/z* calcd. for C$_{40}$H$_{33}$O$_2$ 545.2475, found 545.2483.

# ■ ASSOCIATED CONTENT

**ⓢ Supporting Information.** $^1$H and $^{13}$C NMR spectra for all compounds, Eyring plots for the kinetic studies for *cis*- and *trans*-**5**, and $^1$H NMR spectra after photochemical and thermal isomerization experiments for molecular motor *cis*- and *trans*-**5**. This material is available free of charge via the Internet at http://pubs.acs.org.

# ■ AUTHOR INFORMATION

**Corresponding Author**
*E-mail: b.l.feringa@rug.nl.

# ■ ACKNOWLEDGMENT

## ■ REFERENCES

(1) (a) De Rosier, D. J. *Cell* **1998**, *93*, 17–20. (b) Kinosita, K.; Yasuda, R.; Noji, H.; Ishiwata, S.; Yoshida, M. *Cell* **1998**, *93*, 21–24. (c) Mahadevan, L.; Matsudaira, P. *Science* **2000**, *288*, 95–99. (d) van den Heuvel, M. G. L.; Dekker, C. *Science* **2007**, *317*, 333–336. (e) Schliwa, M., Ed. *Molecular Motors*; Wiley-VHC: Weinheim, 2003.

(2) Macnab, R. M.; Aizawa, S.-I. *Annu. Rev. Biophys. Bioeng.* **1984**, *13*, 51–83.

(3) (a) Vale, R. D.; Milligan, R. A. *Science* **2000**, *288*, 88–95. (b) Kodera, N.; Yamamoto, D.; Ishikawa, R.; Ando, T. *Nature* **2010**, *468*, 72–76.

(4) Boyer, P. D. *Annu. Rev. Biochem.* **1997**, *66*, 717–749.

(5) (a) Browne, W. R.; Feringa, B. L. *Nat. Nanotechnol.* **2006**, *1*, 25–35. (b) Kay, E. R.; Leigh, D. A.; Zerbetto, F. *Angew. Chem., Int. Ed.* **2007**, *46*, 72–191. (c) Iwamura, H.; Mislow, K. *Acc. Chem. Res.* **1988**, *21*, 175–182.

(6) (a) Balzani, V.; Credi, A.; Raymo, F. M.; Stoddart, J. F. *Angew. Chem.* **2000**, *112*, 3484–3530. *Angew. Chem., Int. Ed.* **2000**, *39*, 3348–3391. (b) Kinbara, K.; Aida, T. *Chem. Rev.* **2005**, *105*, 1377–1400. (c) Kottas, G. S.; Clarke, L. I.; Horinek, D.; Michl, J. *Chem. Rev.* **2005**, *105*, 1281–1376. (d) Tian, H.; Wang, Q.-C. *Chem. Soc. Rev.* **2006**, *35*, 361–374. (e) Balzani, V.; Credi, A.; Silvi, S.; Venturi, M. *Chem. Soc. Rev.* **2006**, *35*, 1135–1149. (f) Saha, S.; Stoddart, J. F. *Chem. Soc. Rev.* **2007**, *36*, 77–92. (g) Champin, B.; Mobian, P.; Sauvage, J.-P. *Chem. Soc. Rev.* **2007**, *36*, 358–366. (h) Feringa, B. L. *J. Org. Chem.* **2007**, *72*, 6635–6652.

(7) Feringa, B. L., Ed. *Molecular Switches*; Wiley-VCH: Weinheim, 2001.

(8) (a) Special issue on molecular machines: *Acc. Chem. Res.* **2001**, *34*, 410−522. (b) Balzani, V.; Credi, A.; Venturi, M. *Molecular Device and Machines − Concepts and Perspectives for the Nanoworld*; Wiley-VCH: Weinheim, 2008. (c) Sauvage, J.-P., Ed. *Molecular Machines and Motors*; Springer: New York, 2001.

(9) (a) Koumura, N.; Zijlstra, R. W. J.; van Delden, R. A.; Harada, N.; Feringa, B. L. *Nature* **1999**, *401*, 152–155. (b) Koumura, N.; Geertsema, E. M.; van Gelder, M. B.; Meetsma, A.; Feringa, B. L. *J. Am. Chem. Soc.* **2002**, *124*, 5037–5051. (c) van Delden, R. A.; ter Wiel, M. K. J.; Pollard, M. M.; Vicario, J.; Koumura, N.; Feringa, B. L. *Nature* **2005**, *437*, 1337–1340. (d) Leigh, D. A.; Wong, J. K. Y.; Dehez, F.; Zerbetto, F. *Nature* **2003**, *424*, 174–179. (e) Hernández, J. V.; Kay, E. R.; Leigh, D. A. *Science* **2004**, *306*, 1532–1537.

(10) (a) Kelly, T. R.; De Silva, H.; Silva, R. A. *Nature* **1999**, *401*, 150–152. (b) Fletcher, S. P.; Dumur, F.; Pollard, M. M.; Feringa, B. L. *Science* **2005**, *310*, 80–82.

(11) ter Wiel, M. K. J.; van Delden, R. A.; Meetsma, A.; Feringa, B. L. *J. Am. Chem. Soc.* **2003**, *125*, 15076–15086.

(12) (a) Klok, M.; Boyle, N.; Pryce, M. T.; Meetsma, A.; Browne, W. R.; Feringa, B. L. *J. Am. Chem. Soc.* **2008**, *130*, 10484–10485. (b) Pollard, M. M.; Meetsma, A.; Feringa, B. L. *Org. Biomol. Chem.* **2008**, *6*, 507–512.

(13) Vicario, J.; Walko, M.; Meetsma, A.; Feringa, B. L. *J. Am. Chem. Soc.* **2006**, *128*, 5127–5135.

(14) (a) Eelkema, R.; Pollard, M. M.; Vicario, J.; Katsonis, N.; Ramon, B. S.; Bastiaansen, C. W. M.; Broer, D. J.; Feringa, B. L. *Nature* **2006**, *440*, 163. (b) Eelkema, R.; Pollard, M. M.; Katsonis, N.; Vicario, J.; Broer, D. J.; Feringa, B. L. *J. Am. Chem. Soc.* **2006**, *128*, 14397–14407.

(15) ter Wiel, M. K. J.; van Delden, R. A.; Meetsma, A.; Feringa, B. L. *Org. Biomol. Chem.* **2005**, *3*, 4071–4076.

(16) Fox, J. M.; Huang, X.; Chieffi, A.; Buchwald, S. L. *J. Am. Chem. Soc.* **2000**, *122*, 1360–1370.

(17) Billingsley, K.; Buchwald, S. L. *J. Am. Chem. Soc.* **2007**, *129*, 3358–3366.

(18) All of the UV−vis and NMR spectroscopic studies were performed on racemates.

(19) Because of the low rate of thermal inversion from unstable *cis*-**5** to stable *cis*-**5**, the solvent was changed from DCM to DCE to allow temperatures above the boiling point of DCM (40 °C).

(20) (a) van Delden, R. A.; ter Wiel, M. K. J.; de Jong, H.; Meetsma, A.; Feringa, B. L. *Org. Biomol. Chem.* **2004**, *2*, 1531–1541. (b) Ruangsupapichat, N.; Pollard, M. M.; Harutyunyan, S. R.; Feringa, B. L. *Nature Chem.* **2011**, *3*, 53–60.

(21) Geertsema, E. M.; van der Molen, S. J.; Martens, M; Feringa, B. L. *Proc. Natl. Acad. Sci. U.S.A.* **2009**, *106*, 16919–16924.

(22) See the Supporting Information for more details.

(23) Schoevaars, A. M.; Kruizinga, W.; Zijlstra, R. W. J.; Veldman, N.; Spek, A. L.; Feringa, B. L. *J. Org. Chem.* **1997**, *62*, 4943–4948.

(24) This graph shows the region of the spectrum in which the absorptions are that were used to perform the calculations. These are not the methoxy protons (proton 4, see Figure 5) and its corresponding proton (proton 2), but the other two protons (protons 1 and 5) on the *m*-methoxyphenyl. The latter were used for the calculations because their absorptions had less overlap with other absorptions, which is essential for the accuracy of the calculations.

(25) (a) Sanders, J. K. M.; Hunter, B. *Modern NMR Spectroscopy; A Guide for Chemists*; Oxford University Press: Oxford, 1987. (b) Friebolin, H. *Basic One- and Two Dimensional NMR Spectroscopy*; VHC: New York, 1998. (c) Ernst, R. R.; Bodenhausen, G.; Wokaun, A. In *Principles of Nuclear Magnetic Resonance Spectroscopy in One and Two Dimensions*; Clarendon Press: Oxford, 1987.

(26) More details on the 2D-EXSY measurements and calculations can be found in the experimental general remarks section.

(27) (a) Bodenhausen, G.; Ernst, R. R. *J. Am. Chem. Soc.* **1982**, *104*, 1304–1309. (b) Macura, S.; Ernst, R. R. *Mol. Phys.* **1982**, *41*, 95–117. (c) Jeener, J.; Meier, B. H.; Bachmann, P.; Ernst, R. R. *J. Chem. Phys.* **1979**, *71*, 4546–4553.